Reference: *Biol. Bull.* **170:** 461–480. (June, 1986)

STRUCTURE AND OPTICS OF OMMATIDIA FROM EYES OF STOMATOPOD CRUSTACEANS FROM DIFFERENT LUMINOUS HABITATS

HELGA SCHIFF, RAYMOND B. MANNING, AND BERNARD C. ABBOTT

Dipartimento di Informatica, via Valperga Caluso, 37, Università di Torino, 10125 Torino, Italy, Department of Invertebrate Zoology, National Museum of Natural History, Smithsonian Institution, Washington, DC 20560, and Department of Biological Sciences, University of Southern California, Los Angeles, California 90007

Abstract

Shapes and sizes of ommatidia in six genera of stomatopods from different luminous habitats are described. Cornea-cone apertures and acceptance angles have been calculated. The ommatidia belong to the apposition type with fused rhabdoms as in most Malacostraca, but the spindle-shaped cone and the transparent wedges under the cornea are acquisitions of stomatopods. The same is true for rhabdom specializations, especially the thin undulated rhabdoms in ommatidia of the six-row middle band of the Gonodactyloidea, that divides the eye in two halves. Several regions can be distinguished in stomatopod eyes by differences in shapes, sizes, and proportions of their ommatidia and by the skewing pattern along the columns of ommatidia. As more light becomes available in the habitat, apertures and acceptance angles seem to decrease mainly by increasing the lengths of the cones.

Introduction

Ommatidia, their optics, visual fields, eye maps, and other parameters in insect and crustacean eyes have been described for many species (extensive surveys are given in the following articles: Kunze, 1979; Snyder, 1979; Land, 1981b; Wehner, 1981; Shaw and Stowe, 1982). The ommatidia and eyes of stomatopod crustaceans have several characteristics which differ from any other compound eye. We have started several lines of research on the structure and function of these eyes in an attempt to analyze possible integrating and range-finding mechanisms. Trying to correlate the various parameters of the single ommatidium and the ensemble of ommatidia with the luminous environments of the species, we realized that our knowledge of the luminosity in the microhabitats and of the daily activity cycles is limited. In fact, if evolutionary adaptations occur, they are not obvious and not coherent throughout the genera analyzed. In this paper we describe structure and optics of the single ommatidium of the following species:

Bathysquilla crassispinosa (Manning, 1961) (Bathsquillidea, 500+ m depth).
Echinosquilla guerini (White, 1861) (Protosquillidae, 100 m depth).
Squilla mantis (Linnaeus, 1758) and *S. empusa* Say, 1818 (Squillidae, generally less than 100 m depth).
Hemisquilla ensigera (Owen, 1832) (Hemisquillidae, *ca.* 20 m depth).
Gonodactylus spp. (several species, Gonodactylidae, shallow, tropical, coastal waters).
Pseudosquilla ciliata (Fabricius, 1787) (Pseudosquillidae, shallow, tropical, coastal waters).

Received 12 November 1985; accepted 25 March 1986.

Materials and Methods

Dimensions of the components of ommatidia were measured from photographs of living razor-cut eyes and from histological sections, primarily from unstained sections of eyes fixed in glutaraldehyde. A Leitz Orthoplan with or without interference optics and uv-fluorescence was used to study the sections.

We calculated the acceptance angle (which determines the visual field) according to Snyder (1979) (see below). We do not know the refractive indices of the components of the optical equipment of the ommatidia. Therefore we calculated the acceptance angle for two mean values: 1.5 and 1.4. The former value was used by Horridge and Duelli (1979). We have considered 1.4 as the lower limit because the refractive index of seawater is around 1.34. Obviously our calculations do not give precise values for the acceptance angles. But the changes determined by different dimensions of the optical system are much larger than those caused by varying refractive indices (Table II). The mean value of the refractive index of the whole optical equipment presumably would be between the two values used in our calculations. Refractive indices measured in other arthropods lie between 1.35 and 1.55. The refractive index does not vary within the cone. It does vary in the corneal layers and between cornea, the corneagenous cells, and the cone. Furthermore, the calculations following Snyder (1979) do not consider the curvatures of the corneal surfaces. It seems impossible to calculate the acceptance angle precisely considering the refraction by the cornagenous cells and the cone structure. Thus, our calculations seem to be a reasonable approximation until electrophysiological measurements are available.

The apertures, *i.e.,* the angle within which light would be admitted to the ommatidium, were calculated trigonometrically from the facet diameter and the distance between the corneal surface and the distal tip of the rhabdom. The same angle results from the contour of a longitudinal cone section. We also measured it by looking through the cornea-cone unit at an image at a distance of 3 cm and one at 1 m from the eye. The portion of the image that is transmitted through the unit indicated an aperture corresponding to the calculated aperture. Obviously, this does not mean that all light entering also will be transmitted into the rhabdom. All measurements were taken from eyes adapted to bright light. In *Squilla,* the cone widens and the rhabdom lengthens during dark adaptation (Schiff, 1974).

Comparative pseudopupil observations are described in Abbott *et al.* (1984). Because of the complex structure and optics of stomatopod ommatidia, pseudopupil measurements do not supply information about either the acceptance angle or the aperture, but only about the distribution of optical axes.

Ommatidia parallel to the middle band of specialized ommatidia are arranged in *rows;* sequences of ommatidia perpendicular to the rows are called *columns.* The parts of the cornea furthest away from the middle band are the sides and between these and the middle band are the submedian parts of the eye.

Results

Stomatopods, predatory Crustacea who catch their prey with a violent strike (Caldwell and Dingle, 1976), have eyes designed presumably for monocular and binocular range-finding (Schiff *et al.,* 1985). The eyes are divided into two halves by a middle band (Demoll, 1909; Schiff, 1963, 1976; Horridge, 1978) of either two or six rows of ommatidia in the species described here. Along the column the first 3–10 ommatidia on each side of the middle band are skewed towards the middle band. In this way axes of skewed ommatidia in one half of the eye cross those from the ommatidia in the opposite half. *Squilla* and *Echinosquilla* from a dim habitat have approximately

cylindrical corneas divided by two rows of middle ommatidia in a groove in the former species and six rows in the latter. *Odontodactylus, Hemisquilla, Gonodactylus,* and *Pseudosquilla* from a medium to bright environment have spherical to elliptical corneas with six rows of middle ommatidia which in *Odontodactylus* and *Gonodactylus* form a crest and in *Hemisquilla* and *Pseudosquilla* a slight depression.

Although many stomatopod species live in dim to dark environments where superposition eyes would be more suitable to catching light, stomatopods possess apposition eyes. To compensate for this, the corneal facets, cones, and rhabdoms are large. Most facets are hexagonal, but square, pentagonal, and rectangular facets occur in certain regions of the eye (see below). The typical shape of a stomatopod ommatidium is shown in Figure 1. Average sizes and shapes of ommatidia from five species from different luminous habitats are drawn in Figure 2.

Four categories of ommatidia can be distinguished by the relative dimensions of the components and by their position in the eye: ommatidia from the sides, the submedian surfaces, the middle band, and skewed ommatidia on each side of the middle band.

From the middle towards the sides, ommatidia diminish in size. At the sides the cones are small or missing. These ommatidia provoke attention position (Demoll, 1909; Schiff, 1963) of eyes and striking appendages.

The shapes of ommatidia are similar in all stomatopods except for the middle ommatidia described below. Sizes and proportions instead vary within one eye in different regions. For the same regions of the eye within one species these differ according to age, *i.e.*, the size of the individual. Sizes and proportions also differ between eyes of different genera (Fig. 2 and Table I). We did not find a clear and coherent relationship between environmental light and dimensions, acceptance angles, and cone apertures. We, therefore, calculated ratios of the various parameters (Table III). But these also do not relate coherently to ambient light conditions. In the tables the species are ordered from least light available (*Echinosquilla*) to very bright (*Gonodactylus* and *Pseudosquilla*). As can be seen, neither dimensions of ommatidia, nor angles of apertures of cones and rhabdoms, nor ratios change coherently with the availability of light. The total number of ommatidia increases, possibly with the availability of light or with the size of the species, being approximately 1500 in *Echinosquilla,* 4000 in *Squilla,* 8000 in *Hemisquilla,* 10,000 in *Odontodactylus,* but only about 5500 in *Gonodactylus.*

Ommatidia in the submedian eye parts

Corneal facets. Corneal facets are hexagonal in all regions of the cornea except for the middle bands and adjacent rows of ommatidia.

The cornea in all stomatopods is composed of many refracting layers (each 1.7 μm thick in *Odontodactylus*). In *Odontodactylus* and *Hemisquilla* strongly refracting double layers have been observed (Fig. 3) at the inner as well as the outer surface of the corneal facet. The distance between the peripheral double layer and the main part of the cornea is 4.3 μm in the center of the facet and 2.3 μm at the transition zone with the neighboring facet. The separation within the double layer is 0.3 μm.

The outer surface curvature of the facets varies within each eye and between genera. Species from a bright environment, such as species of *Odontodactylus, Gonodactylus,* and *Pseudosquilla* have relatively flat outer surfaces of the corneal facets, while *Echinosquilla, Squilla,* and *Hemisquilla* (dark, dim, and medium light habitats) have strongly convex outer facet surfaces. A measure of convexity is given in Figure 2 and Table I showing the thickness of the corneal facet (distal to proximal surface) in the

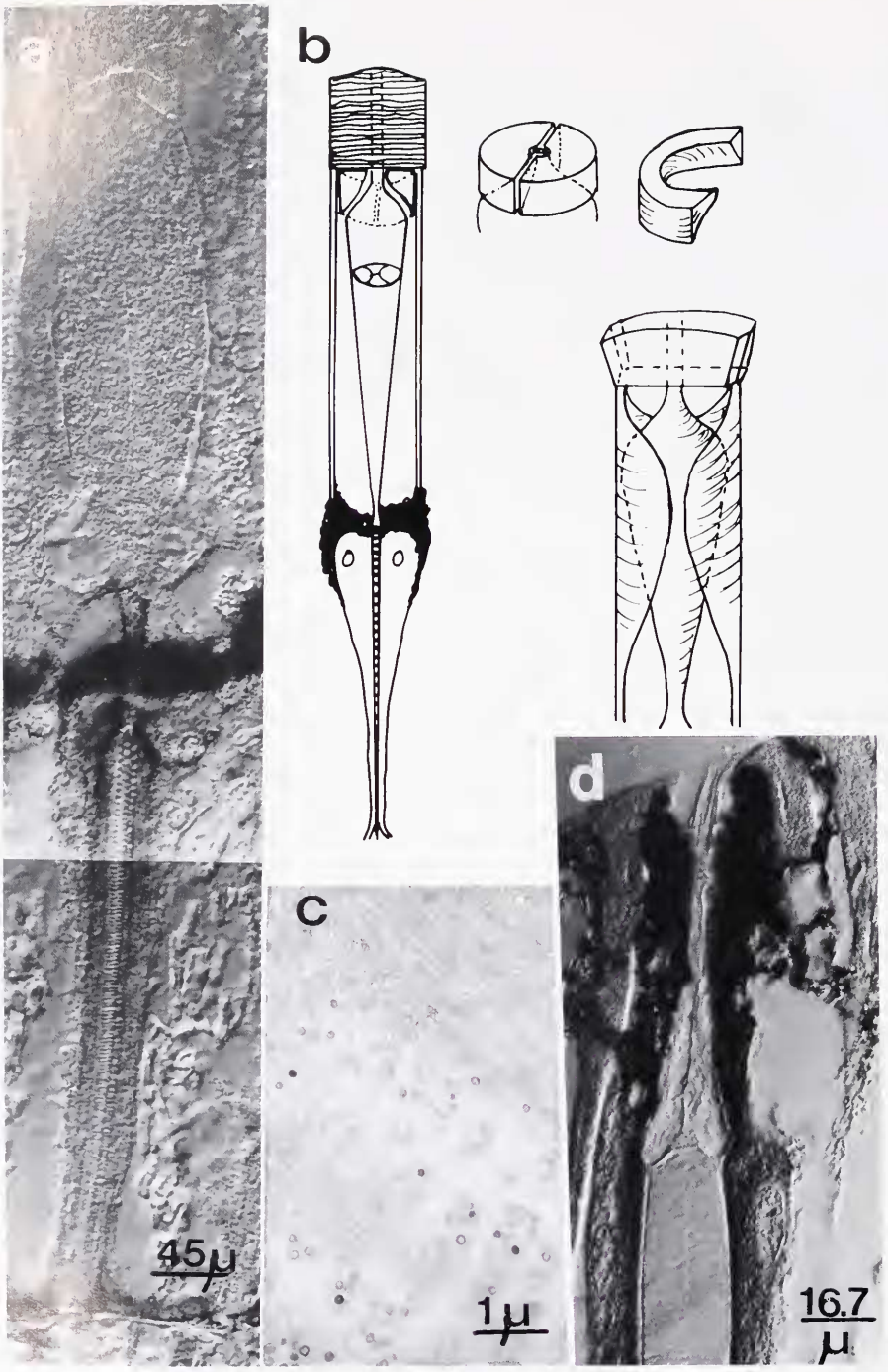

FIGURE 1. The stomatopod ommatidium: (a) an ommatidium of *Pseudosquilla ciliata*, unstained section; (b) diagram of an ommatidium of *Odontodactylus scyllarus* and on the right: the transparent wedges formed by the corneagenous cells and the transparent membranes formed by the accessory pigment cells surrounding the cone; (c) electron microscope photograph tangential to the rhabdom surface from the eye of *Squilla mantis*. The lower part of the photo shows the regular pattern of bridges and columns stretching between the thin layer on the rhabdom surfaces and the main bulk of the retinular cells. (d) Cone-rhabdom junction in an ommatidium of *Squilla mantis* (unstained). Bars and numbers indicate micrometers.

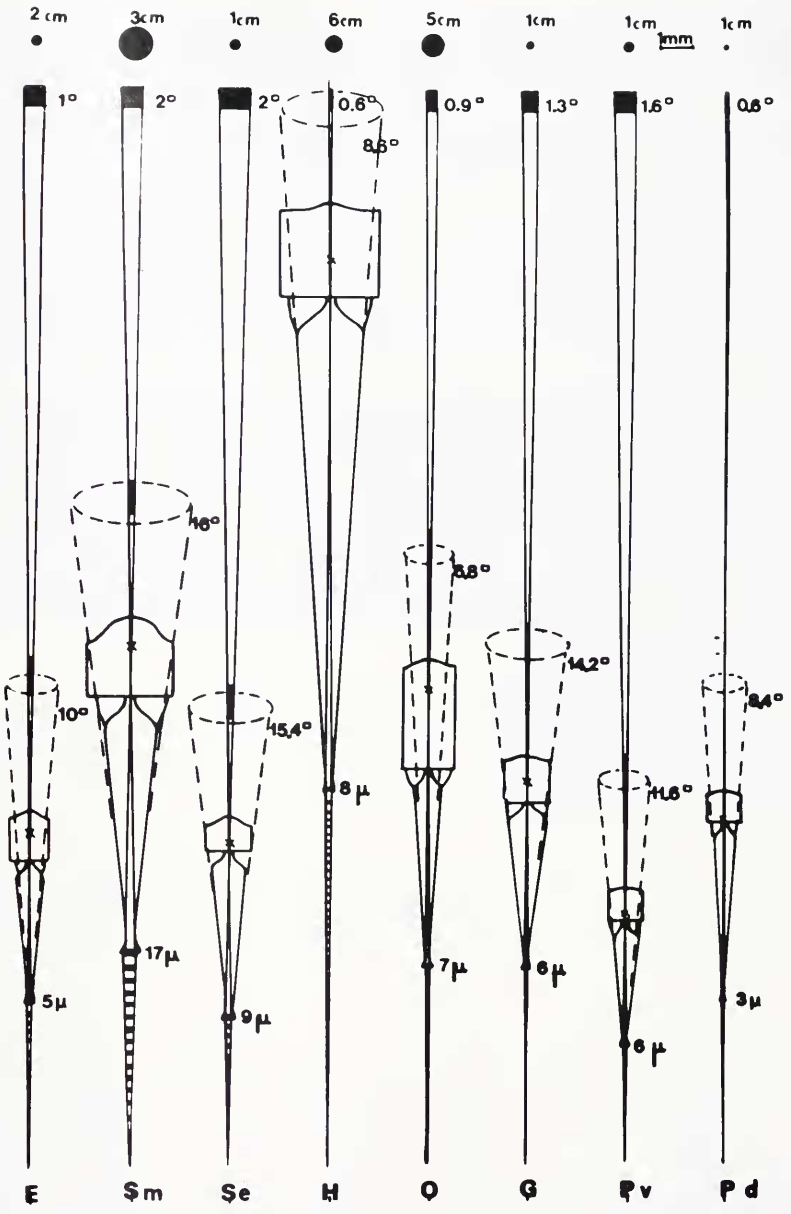

FIGURE 2. Ommatidia of: E: *Echinosquilla guerini;* Sm: *Squilla mantis;* Se: *Squilla empusa;* H: *Hemisquilla ensigera;* O: *Odontodactylus scyllarus;* G: *Gonodactylus,* posterior ommatidium. The frontal ommatidia are similar in dimensions to the frontal ones in *Pseudosquilla* Pd. Pv: posterior and Pd: anterior ommatidia of *Pseudosquilla.* Indicated in micrometers are the diameters of the distal rhabdoms; in degrees on top: acceptance angles, in the middle (dashed lines) the cornea-cone apertures. Above the ommatidia the visual fields are shown at the indicated distances from the cornea together with the scale for the visual fields. Distances chosen are those at the approximate striking distances of the species.

TABLE I

Dimensions of components of ommatidia in micrometers

	Facet diameter		Corneal thickness		Cone maximum diameter		Cone length		Rhabdom maximum diameter		Rhabdom length	
	mi	si	mid.	mar.	mi	si	mi	si	mi	si	mi	si
Echinosquilla	57		73	60	36		208		4.5 ± 0.2		246	
Squilla mantis	128		125	75	77		390		17.8 ± 2.3		323	
Squilla empusa	66 ± 2.7		46 ± 2	38 ± 2	47 ± 3		246 ± 20		9.4 ± 0.3		204 ± 3	
Hemisquilla	110		150	145	100		745		11 ± 0.9	6.8 ± 1.4*	8 ± 2	607 ± 50	570 ± 13
Odontodactylus	115		165		63 ± 18	24* 36	445 ± 89	305 ± 6.6	11 ± 3		6.8 ± 0.2	473 ± 78	302 ± 10
Pseudosquilla													
front	40		40	39	19*	31	270		2.5*		3.1		194
dorsal middle	50		50		40		176 ± 13		11.6 ± 2.1		5.6 ± 1.6	233 ± 14	179 ± 54
Gonodactylus													
front	40	35	60		30	14* 18	230		3			630	
dorsal middle	70		68	65	58.5 ± 6.6		289 ± 13	310* 242	6.3 ± 2.9		6.9 ± 0.4	293 ± 45	295

Hemisquilla, undulated rhabdom: distal diameter = 7.5 μm; main part, diameter = 6 μm; proximal diameter = 1–1.5 μm.
± = value of standard deviation σ.
mi = data for the ommatidia in the middle band.
si = data for the ommatidia to the sides of the middle band, *i.e.,* ommatidia in the submedian parts of the eye.
* = data for the skewed ommatidia adjacent to the middle band.
mid. = middle of corneal facet.
mar. = margins of corneal facet.

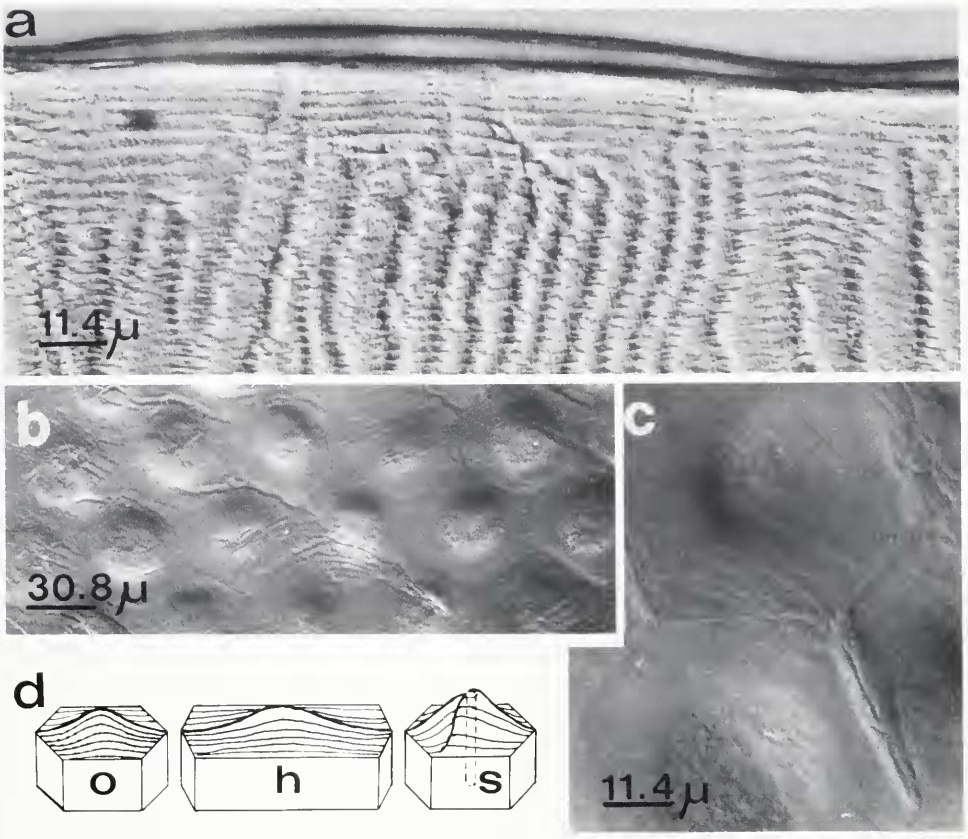

FIGURE 3. The facet surfaces: (a) part of a section through a facet of the *Odontodactylus* eye. Layered structure can be seen and the proximal and distal double layers with different refractive indices (Nomarski optics). (b and c) Tangential sections through facets of the eye of *Pseudosquilla ciliata;* (d) diagrammatic drawings of facets of (o) *Odontodactylus;* (h) *Hemisquilla;* (s) *Squilla.* All sections unstained in polarized light.

center of the facet compared to that at the margins in the different genera. Surface convexity usually is not homogeneous over the facet surface, but a facet is flat in the periphery and rises rather abruptly towards the center (Fig. 3). The surfaces are usually complicated. For example, the facets in *Squilla* show ridges and a small depression in their center. *Hemisquilla* has double ridges, zig-zagging along the rows near the rather flat margins of the facets. In *Gonodactylus* each row of the ommatidia of the middle band has a different shape, and the facet surfaces have different curvatures as well (see also Manning *et al.,* 1984, and, for an extreme case of curvature, Schiff and Manning, 1984).

Cones. Cones in stomatopod eyes have a shape not described for other arthropods. At its distal end the cone slims down abruptly to a 10 μm wide tube, 15 to 20 μm long (*Squilla mantis*) which attaches to the middle of the corneal facet. The space left between the cornea and the widest part of the cone is occupied by the corneagenous cells which form two semicircular wedges around the distal cone extension (Fig. 1). Interference microscopy and observation of the living eye indicate different refractive

indices for the corneagenous cells and the cones. The membranes of cones and corneagenous cells seem to have indices different from those of the intracellular contents.

The cones are built up of four parts delimited by membranes. At its proximal part the cone slims down to a diameter of about 10 μm but then, unlike other arthropod ommatidia, widens again and fits with a concave tip over the convex distal tip of the rhabdom. Four extensions of the cone run down along the rhabdom (Schiff and Gervasio, 1969; Schönenberger, 1977). The maximal diameter of the cones and their lengths are given in Table I, the calculated cone apertures in Table II. The acceptance angle determines the visual field of the ommatidium. The cornea-cone aperture is much larger than the acceptance angle and indicates the solid angle within which light will enter the ommatidium. Part of this light will be reflected or absorbed by pigments at the retinal surface. Light from the small, central visual field will reach the rhabdom. A large aperture means that also oblique rays from the visual field will be funnelled into the rhabdom. It is obvious from Table II that no coherent relationship exists between the cone aperture and ambient light conditions.

The corneal lenslet transmits an image of a wide field corresponding to the cornea-cone aperture (Table II). The image is distorted by spherical aberration. The aberration is corrected in the cones (plus corneagenous cells) which transmit an inverse, side-reversed image with a width corresponding to the cone aperture. The cone focuses light at the level of the rhabdom and little light gets out of the sides of the cone.

In *Gonodactylus* and *Pseudosquilla* the largest surface of the cornea is usually kept dorsally, parallel to the ground and aligned with the body axis. Cone and rhabdom sizes and the relative apertures and acceptance angles are quite different for the front and back halves of the cornea. Whereas the backward and upward looking ommatidia in the proximal part of the eye are similar in dimensions and fields to those of dim light species, the forward looking ommatidia in the front part of the eye are long and slim with small visual fields and apertures (Table II).

In the eyes of some species of *Gonodactylus* and in *Pseudosquilla ciliata* the cone layer as a whole is rather transparent so that one can see the whole retinal surface from outside. Light in these cases gets through the cone walls and is then reflected and absorbed by the pigments on and in the distal retina. In other stomatopods the retinal surface is not seen as a whole because most of the light remains within the cones.

The rhabdom. The rhabdom is a typical fused rhabdom as in most Malacostraca. The number and thickness of layers of perpendicular microvilli differs between species: *Squilla mantis* has only 150 layers each 2 μm thick, but *Hemisquilla ensigera* has 1100 to 1200 layers 0.3 μm to 0.5 μm thick. Using electron microscopy, a thin layer of smaller microvilli in *S. mantis* was observed just under the cone tip which continues for the first few layers along the sides of the rhabdom. The small microvilli have a diameter of only half that of the normal (1000 Å) microvilli.

Retinular cells. Seven retinular cells surround the rhabdom and exit through the basement membrane. Here they lose their pigment (brown in the living eye) and become first order nerve fibers. In *Gonodactylus* these last are still pigmented for some 30–40 μm. Around the retinular cells are the accessory pigment cells (black). The retinal surface in all stomatopod eyes is covered with white, oily droplets. The white pigment is also contained in vesicles in the distal tips of the accessory pigment cells. The vesicles have openings towards the retina surface through which the pigment exits. A green, glittering, crystalline, strongly light-reflecting pigment lies on the retinal surface evenly distributed over the whole surface. In *Hemisquilla* the green and white pigments are concentrated only near the lateral margins with the stalk. The fifth pigment common

TABLE II

Acceptance angles and cornea-cone apertures

	Micron focal length f n = 1.5 (n = 1.4)			*Degrees* acceptance angles n = 1.5 (n = 1.4)			*mm* diameter of vis. field of 3 cm distance			of:	*cm* diam. vs. field at distance			*cm* vis. field of diam. 0.3 mm at distance of			*Degrees* cornea-cone aperture		
	mi		si	mi		si	mi		si		mi		si	mi		si	mi		si
Echinosquilla		251 (269)			1.03 (0.96)			0.5		2		0.3			1.9			10	
Squilla mantis		461 (493)			2.2 (2.07)			1.0		3		1.0			0.8			16	
Squilla empusa		261 (279)			2.08 (1.93)			0.98		1		0.3			0.9			15.4	
Hemisquilla		799 (857)		0.8 (0.74	0.5* 0.46*	0.6 0.54)	0.4	0.2*	0.3	6	0.8	0.46*	0.54	2.4	3.9*	3.3		8.6	
Odontodactylus	544 (584)		420 (450)	1.2 (1.08)		0.9 (0.87)	0.6		0.4	5	0.9		0.7	1.6		2.1	10.4	2.4*	6.8
Pseudosquilla																			
front	297		277		0.52* (0.48)	0.64 (0.57)		0.24*	0.3	1		0.08*	0.1		3.7*	3			8.4
dorsal middle	253 (216)		197	2.6 (3.08)		1.6 (1.49)	1.2		0.8	1	0.4		0.3	0.7		1.2	12.6		11.6
Gonodactylus																			
front		311		0.57	0.37*	0.5		0.26		1		0.17			1.7			10	
dorsal middle	328 (342)		280 (297)	1.1 (1.06)		1.3 (1.2)	0.5		0.6	1	0.2		0.2	1.7		1.5	12		14.2

mi, si, * as in Table I.

TABLE III

Dimensions of components of ommatidia

	Length of cone length of rhabdom		*Length of cornea + cone* facet diameter		*Rhabdom length* rhabdom diameter		*Cornea-cone aperture* acceptance angle	
	mi	si	mi	si	mi	si	mi	si
Echinosquilla	0.9		4		54.7		10	
Squilla mantis	1.2		3.6		18		7	
Squilla empusa	1.0		3.7		21.7		7	
Hemisquilla	1.2	1.3	6.6		55	83* 71	11	17* 14
Odontodactylus	0.9	1.0	4.7	4.7	43	44	9	8
Pseudosquilla								
front	1.4		8		67		13	
dorsal middle	0.8	1.0	4.4		20	32	5	7
Gonodactylus								
front	0.4		17	20	210		20	
dorsal middle	1.0	0.8	4.5		47	48	11	11

mi, si, * as in Table I.

to all stomatopods is bright red and crystalline. The crystals are contained in threadlike structures (Schiff and Gervasio, 1969; Schönenberger, 1977).

A thin (2.3–0.3 μm) layer of retinular cells adheres to the rhabdom. This layer is connected to the main bulk of the cells by cytoplasmic bridges and columns (0.2 μm wide, 0.6 μm long) all enveloped by the cell membrane and distributed in a very regular pattern (Fig. 1) (for *S. mantis* see Schiff and Gervasio, 1969). Therefore there is an apparently empty space between the rhabdom and the bulk of the retinular cells. Similar columns have been found in other Crustacea (Shaw and Stowe, 1982) and seem to be present in all stomatopod ommatidia (except in the 'cube-thread' rhabdom, see below).

Ommatidia in the middle band and skewed ommatidia adjacent to the middle band have different structures and we will describe them in a separate chapter.

Ommatidia in the central part of the eye

All the ommatidia in the *Squilla* eye are similar in shape but those in the two rows of the middle groove are slightly larger. In contrast, the ommatidia in the six rows of the middle band of the spherical and the elliptical eye of other genera are distinctly different from all the other ommatidia. Also the skewed ommatidia in the first four to five rows on each side of the middle band show differences with respect to other ommatidia, mainly because they are longer and slimmer.

The six-row middle band (Fig. 4)

Cornea. In *Gonodactylus* the corneal facets in the middle band have different surface curvatures for each row, and thus bulge out to different degrees. *Hemisquilla, Gonodactylus, Pseudosquilla,* and, especially *Odontodactylus,* have rectangular surface facets with their longer dimensions across the middle band (*Odontodactylus:* 150 μm across, 80 μm along the middle band). In *Gonodactylus* facets also differ in size in the different rows. There are two rows of ommatidia with large facets (30 μm $\times$ 14 μm), one with larger (33 μm $\times$ 18 μm), one with smaller (24 μm $\times$ 15 μm) and finally one with larger (30 μm $\times$ 18 μm) facets. The corneal facets of the first 3 to 5 rows of

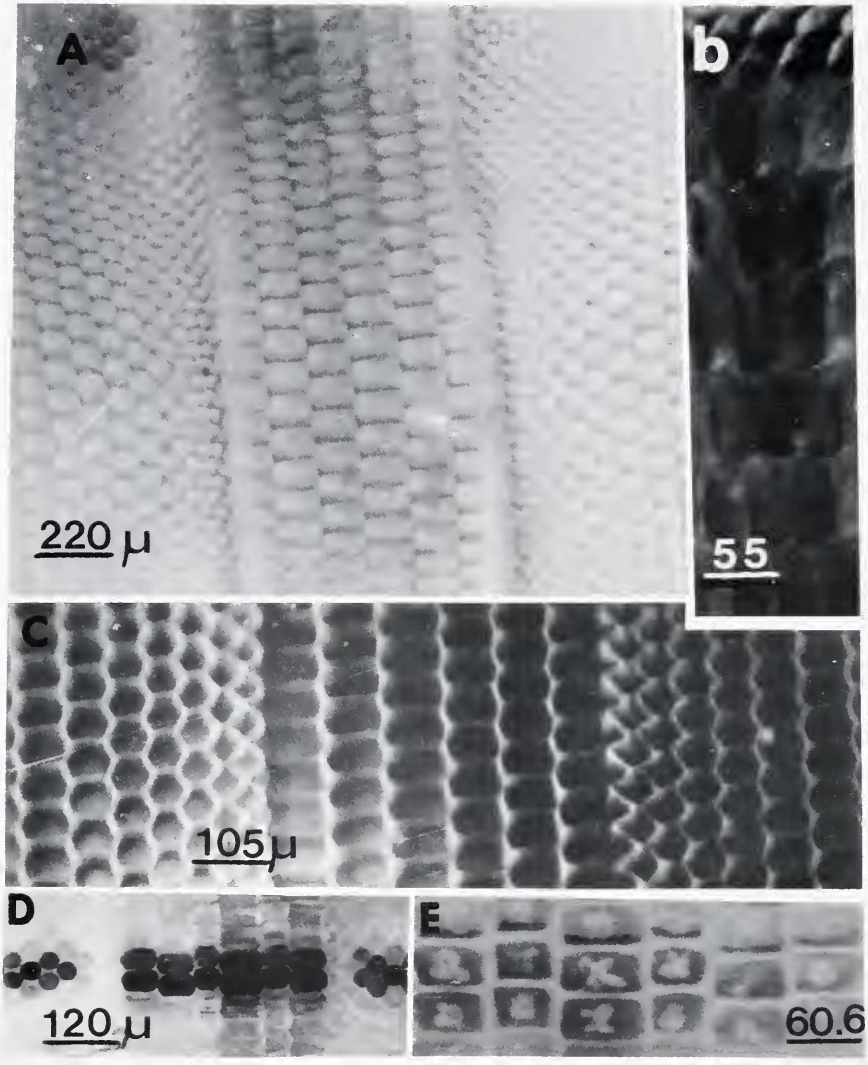

FIGURE 4. Facets in the middle band: (a and b): in *Odontodactylus;* (c): in *Hemisquilla* (focusing slightly below the surface); (d and e): in *Gonodactylus.* In (e) notice the light patterns in the depth of the pseudopupil. These patterns can be seen in most stomatopod pseudopupils, but have different characteristic shapes and sizes in different species. In *Gonodactylus* they are particularly large and cloverleaf shaped.

ommatidia adjacent to the middle band are small (Table I) and square, then gradually grow and become pentagonal and finally hexagonal as are all the remaining facets. The small facets of the three to six rows adjacent to the middle band belong to skewed ommatidia with optical axes convergent between the two halves of the eye.

Cones have the same shape, though not the same dimensions, everywhere.

The rhabdoms and retinular cells. The rhabdoms of five of the six rows of middle ommatidia are considerably larger than in the other ommatidia and also differ in shape. Across the middle band the first two rows of ommatidia have rhabdoms with

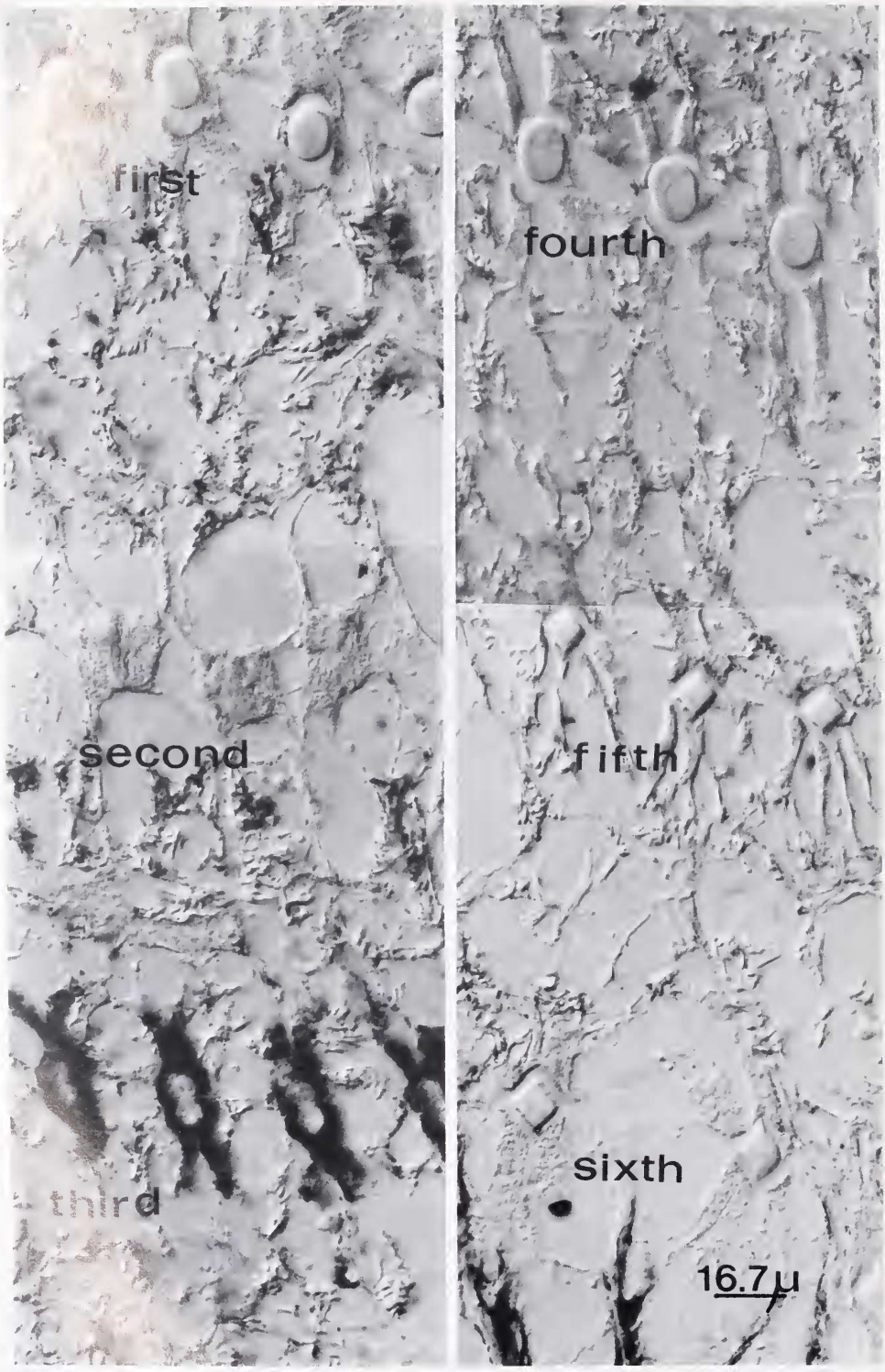

FIGURE 5. Cross section (unstained) through the rhabdoms in the middle band of the eye of *Odontodactylus*. The darkly pigmented ommatidia (third row from the top) are the "cube-thread" ommatidia.

square sections (but larger than elsewhere in the eye). This is followed by one row with round cross sections, one row with a 'cube-thread' (see below) rhabdom, one row with round cross sections and finally one with square cross sections (Fig. 5).

The retinular cells in ommatidia in the middle band are larger than those in the remaining part of the eye. The amount of pigment in the retinular cells is small and different for each row in the middle band. It is concentrated mainly around the rhabdoms in the light-adapted state. The pigmentation varies also with species and genus.

In one row next to the 'cube-thread' ommatidia in the eyes of *Gonodactylus* and *Pseudosquilla*, a small section between cone and rhabdom shows up bright red (light filter?) in unstained, glutaraldehyde-fixed preparations.

The 'cube-thread' rhabdom. A rhabdom has been observed in *Hemisquilla* and *Odontodactylus* which we have called the 'cube-thread' rhabdom (Figs. 6, 7), referring to its appearance in sections: 3 μm wide cubes at regular distances, connected by a thin (0.1 μm) thread. A reconstruction from serial sections shows it to be an undulated rhabdom which in a section appears as a thread beaded with little cubes at regular distances. The cubes are cross sections through the 3 to 6 μm wide rhabdom, while the threads are a small unpigmented space between two neighboring retinular cells. As the retinular cells are heavily pigmented, the spaces between neighboring cells show up lighter. We think that the undulation of the rhabdom, and only of the rhabdom but not the retinular cells, is not an artifact for the following reasons: if the zig-zagging were an artifact caused by fixation, a living and straight rhabdom would be much longer than the available space between cone and basement membrane. Furthermore, the spacing is very regular and a membrane envelopes the rhabdom. At the distal and proximal ends of the rhabdom the undulation can be observed directly (Figs. 6, 7) and the retinular cells are clearly not undulated.

The 'cube-thread' rhabdom seems to be present also in *Gonodactylus* and *Pseudosquilla* and may exist in all eyes with six rows in the middle band.

At the distal end of the ommatidium the retinular cells do not surround the rhabdom up to its junction with the cone but turn away from it more proximally. Therefore, a large part of the distal rhabdom is not covered by pigmented cells and can be easily observed. It is tightly waved (Fig. 6) and enveloped by a membrane which starts at the cone junction. The distal rhabdom is larger and clearly layered (Figs. 6, 7).

Though the proximal rhabdom is surrounded by the retinular cells, it is observed readily because, being thinner and undulated less tightly, all of it fits into a single section (Figs. 6, 7). While the retinular cells are straight, the rhabdom is undulated down to the basement membrane.

Proximal to the basement membrane the axons form small bundles, each bundle running in a different direction. Also, the sub-basement bundling pattern is different from that in the other ommatidia (described for *Squilla mantis* in Schiff *et al.*, 1986a). As shown in Figure 7, each axon from one side of the rhabdom, joins two from the other sides of the rhabdom. The seventh axon from the fourth side of the rhabdom probably also joins one of the bundles, but cannot be seen in the same section. Each bundle then runs in a different direction towards the lamina. While the retinular cells become thin when passing through the basement membrane, they bulge out like a cell proximal to it (Fig. 7). After this significant enlargement they become normal nerve fibers again and gradually loose their pigmentation (Fig. 7).

Visual fields and optical axes of the ommatidia

Table II gives the acceptance angles of the rhabdoms (half width of the sensitivity curve) calculated following Horridge and Duelli (1979) and described in more detail

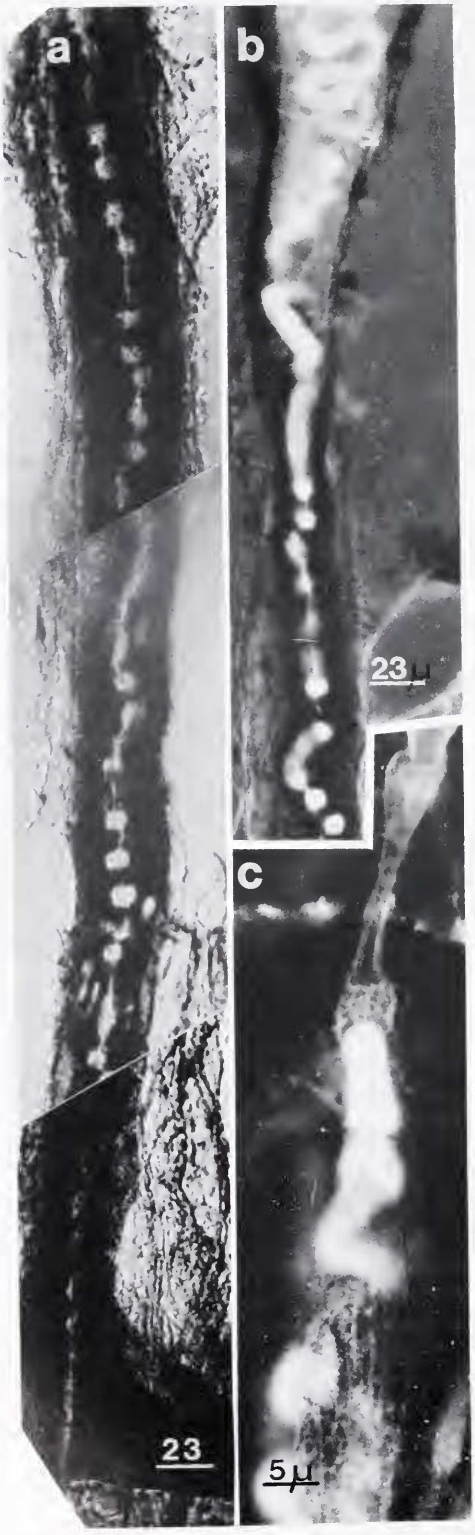
a
b
23μ
c
23
5μ

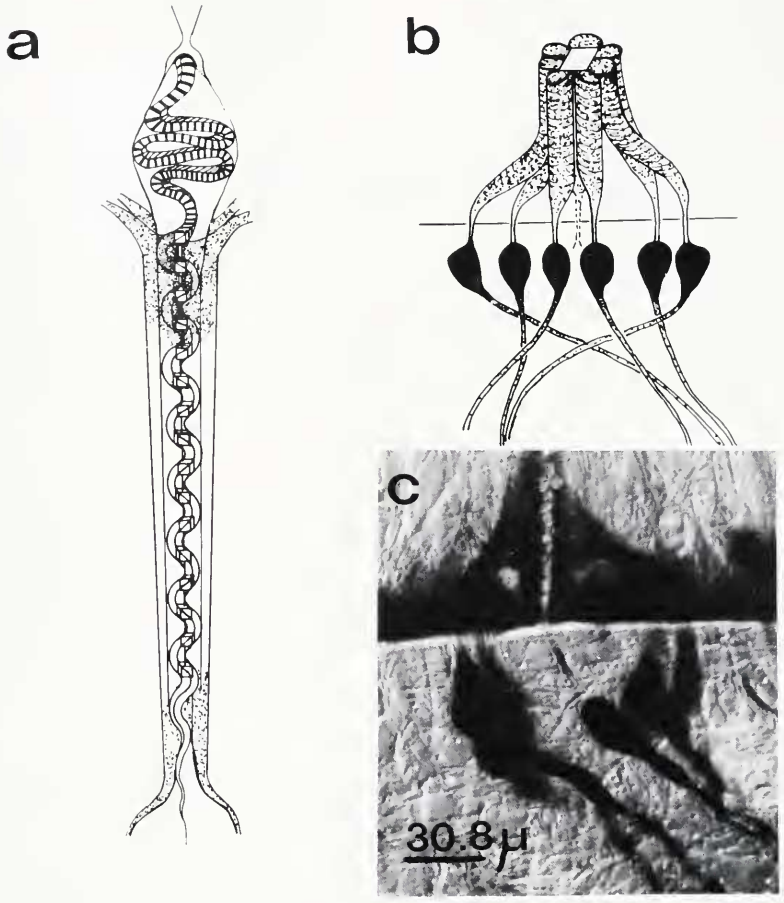

FIGURE 7. (a) Diagram reconstructed from serial sections of the "cube-thread" rhabdom. The little cubes indicate what is seen in a section like Figure 7a. (b and c) Show the proximal part of the c-t ommatidium with the thin fibers passing through the basement membrane, the cell-like bulging of fibers and the subsequent grouping of first order fibers (unstained section).

in Schiff *et al.*, 1986a). The acceptance angle or half width of the sensitivity curve is given by:

$$(\Delta\rho)^2 = \left(\frac{\lambda}{D}\right)^2 + \left(\frac{d}{f}\right)^2$$

where $\frac{\lambda}{D}$ represents the diffraction component (λ = wavelength of light, D = diameter of the corneal facet). In stomatopods the facets are so large that the $\frac{\lambda}{D}$ component can

FIGURE 6. (a) The "cube-thread" rhabdom (unstained); (b) the distal, layered part of the c-t rhabdom surrounded by a membrane; (c) the cone juntion with the c-t rhabdom. In the lower part of the figure the rhabdom-surrounding membrane is in focus. (b and c) Photographed in ultraviolet light. The rhabdoms and cones are fluorescent in UV light especially in preparations fixed in glutaraldehyde.

be neglected and the acceptance angle calculated from the anatomical component $\frac{d}{f}$, d is the diameter of the distal rhabdom surface and f is the value of the lens system calculated from:

$$f = \frac{n_0}{n_1} \text{ times (distance from corneal surface to distal rhabdom)}$$

(For the theoretical treatment of the optics in arthropod eyes see Snyder, 1979.)

n_0–refractive index of seawater taken as 1.34.
n_1–refractive index of cornea and cone. As we do not yet know the refractive indices of the components of the optical system the acceptance angles were calculated for mean refractive indices of 1.5 and 1.4 (in brackets) in Table II.

$\frac{d}{f}$ = acceptance angle in radians.

Also indicated in Table II are the diameters of the visual fields at a distance of 3 cm and at the estimated striking distance of the species. These values are compared for the different genera in Figure 2, where the cornea-cone apertures also are indicated. With the exception of *Echinosquilla* and considering only the front part of the eyes in *Pseudosquilla* and *Gonodactylus,* we find that the acceptance angles diminish as more light becomes available to the species. No large differences between species of the same genus have been found.

Because the functioning of a compound eye is determined by the properties and orientation of the individual ommatidia as well as by the ensemble of ommatidia and by their neural connectivity, we have studied the patterns of skewing of optical axes and part of the neuroanatomy. Skewing of ommatidia was studied both by pseudopupil observations and by histological measurements. No significant deviation occurs between optical and anatomical axes (Schiff *et al.,* 1985). The neuroanatomy of *Squilla mantis* has been described (Hanström, 1924; Schiff, 1976; Strausfeld and Nässel, 1981; Schiff *et al.,* 1986a) and from preliminary results it seems that it is not much different from the other stomatopods.

Along the columns of the eyes of all stomatopods are three long sections—one in each hemisphere of the eye and one in the middle band—in which optical axes are nearly parallel to each other, *i.e.,* with zero interommatidial angles, giving rise to the typical stomatopod triple pseudopupil (Abbott *et al.,* 1984). Optical axes of these ommatidia are perpendicular to the surface of the middle band and visual fields overlap strongly. The ommatidia separating the three sections from each other are skewed, to a different degree for each row, towards the middle band (Schiff *et al.,* 1985, 1986b; Schiff and Candone, 1986).

Along the rows, angles between two and five degrees separate the visual fields of the columns from each other in most stomatopod eyes. Smaller acceptance angles usually are associated with smaller interommatidial angles (*Hemisquilla*) and larger acceptance angles with larger interommatidial angles (*Squilla*).

Few large fibers (Tan 2 in Strausfeld and Nässel, 1981; T 3 in our description: Schiff *et al.,* 1986a) run vertically over the lamina, sending horizontal branches between the rows of cartridges, thus forming a horizontal-vertical matrix mirroring the columns

and rows of ommatidia. The horizontal branches contact the cartridges along their path.

Discussion

The different and quite complicated shapes of the facet surfaces, the shapes of the cones, the corneageous cell wedges, and the specializations at the cone-rhabdom junctions make it practically impossible to treat the optics theoretically. However, we know (at least for *Squilla mantis*) from direct observation that an image is transmitted which can be seen throughout the cone, varying only in size. Furthermore, we know that the image is distorted (curved) at the margins of the facet after passing through the corneal lenslet alone. This is corrected after the passage through the wedges of corneagenous cells. These permit the marginal rays to enter the cone. This means that the complex surfaces of the facets, the different refractive indices, and shapes of the components of the optic ensemble constitute an efficient lens system forming a clear image at the rhabdom. Land (1981a) measured refractive indices in cones of deep sea amphipods, and found that their refractive indices change in different parts of the cones. However, in stomatopods the rays may be funnelled to the rhabdom by the wedges without the need for the differential refraction within the cone: different indices in the cornea, wedges, and cones could explain the image formation, and, judging from interference microscopy, indices are, in fact, different.

If we calculate the visual fields of ommatidia of stomatopods we find that they are quite small, the large facets being compensated by long cones. We also find that the solid angle defined by the acceptance angle matches the proximal and distal cone extensions. Thus the paraxial rays would not pass through the wedges but enter the cones directly from the corneal facet. More oblique rays, coming from within the visual field, would pass through the wedges to be focused at the level of the rhabdom. This arrangement would have the advantage of using light within the large solid angle of the cornea-cone aperture (important for animals from dim environments), still preserving a small visual field (important for resolution of moving objects).

The wide facets with large apertures and wide rhabdoms allow a large amount of light to reach and enter the rhabdom. If the rhabdom is long, light passes through more membranes with photopigment than in shorter rhabdoms. Therefore, more light can be absorbed in a long rhabdom. Land (1981a) has shown that the number of photons per second s_a the rhabdom will receive and can absorb from an extended source emitting $L \cdot m^{-2} \cdot s^{-1} \cdot sr^{-1}$ photons is:

$$s_a = L\left(\frac{\pi}{4}\right)^2 \cdot \left(\frac{D}{f}\right)^2 \cdot d^2 \cdot (1 - e^{-kx}) \text{ or approximately:}$$

$= L\,D^2(\Delta\rho)^2$ for long rhabdoms with negligible diffraction, with D = lens diameter, d = rhabdom diameter, f = focal length, k = absorption coefficient, $\Delta\rho = \frac{d}{f}$ = acceptance angle, and x = length of rhabdom. Thus the efficiency of absorption of photons in the rhabdom increases with the diameters of corneal lens and rhabdom and with the length of the rhabdom.

A more efficient use of available light is also achieved by optical and neural pooling. Many visual fields in each column overlap (optical pooling) and the T 3 fiber, found also in *Pandalus* (Nässel, 1975) and amphipods (Land, 1981a), may be responsible for neural pooling, as suggested also by Land (1981b).

In *Gonodactylus* and *Pseudosquilla* ommatidia in the front and back of the eye

differ in their optical properties. While proximal ommatidia have wide acceptance angles and short cones, the distal (front) ommatidia have small acceptance angles, long cones, small apertures, and long thin rhabdoms. It would seem, therefore, that the ommatidia in the back are better suited for a working range in low light intensities and the front ommatidia for bright light ranges. The ommatidia in the back of the eye are looking towards the crevices where the animals hide. The ommatidia in the front are looking forward into the bright light.

From these data it would seem that stomatopods, though sharing apposition eyes with animals from bright habitats, during their evolution may have adapted to dim or dark environments (wide apertures). Those species which successively occupied brighter habitats had to redevelop adaptations to avoid excessive light and saturation of receptors. These adaptations may be filters between the cone and rhabdom (red stoppers in *Gonodactylus*), changing of the proportions (for example increasing the lengths of the cones) and other, more subtle features (for example different refractive indices as in *Pseudosquilla* which might permit light to exit from the cones before reaching the rhabdom).

The meaning and importance of the middle band and its ommatidia still escapes an interpretation. The larger rhabdoms and facets may, in some cases, constitute a foveal region (Horridge, 1978), but for most ommatidia the calculated acceptance angles are not smaller and the interommatidial angles are zero. This is similar to the situation in amphipod eyes and, according to Land (1981a), increases the ability to detect small objects and/or low contrast against a homogenous background. Neuroanatomical and behavioral clues indicate that the middle bands are involved in binocular range-finding for longer distances than the monocular mechanism (Schiff *et al.,* 1985, 1986a, b).

We did not find any discussions in the literature about the optical implications of the different shapes of rhabdoms (for example square against round cross sections). Twisted rhabdoms have been described (Smola and Wunderer, 1981) and treated theoretically (McIntyre and Snyder, 1978), but the cube-thread rhabdom is not twisted but undulated. The cube-thread rhabdoms may constitute reference points for moving targets or adapt the whole eye to the environmental light. Having a very long rhabdom it could absorb more light before getting saturated, or in other words: it would have a wide range between minimum and maximum absorption.

The linear organization of ommatidia which produces the long, thin, triple pseudopupil (Abbott *et al.,* 1984) is repeated in each neighboring column. These columns are separated by interommatidial angles that are greater than the calculated acceptance angles of the individual ommatidia (Table II). It is possible that the enhanced sensitivity of the pooled columnar input coexists with a high resolution in the horizontal direction by suitable inter-columnar neural differentiation. The combination of wide facets with small acceptance angles, as well as the combination of pooled information along the columns *versus* high resolution along the rows, may work together to provide high sensitivity with little loss of resolution.

We hypothesize that the double eye, overlapping fields, and skewing patterns of ommatidia constitute a monocular range-finding device (Schiff *et al.,* 1985). Inputs are integrated in the T 3 fiber and transmitted as the visual cue for the strike used to catch prey. As vertically, along the columns, high sensitivity is achieved by the overlapping fields, an integrative mechanism for range-finding could function also in dim light. But, as the composite fields of columns are separated by inter-ommatidial angles greater than the acceptance angles along the rows, resolution in the horizontal direction may result between the global, integrative range-finders of each column.

ACKNOWLEDGMENTS

We gratefully acknowledge the support of this research by Consiglio Nazionale delle Ricerche/National Science Foundation grants 77.01544.63, 78.02741.63, and 80.02404.02, and NATO grant 1363 to H. Schiff. H.S. also acknowledges support from the Office of Fellowships and Grants, Smithsonian Institution, during her visit in February 1983. The Institute of Anthropology, University of Torino, provided working space and the use of a microscope, and Mr. L. Burzio of that institute printed the photographs.

LITERATURE CITED

ABBOTT, B. C., R. B. MANNING, AND H. SCHIFF. 1984. An attempt to correlate pseudopupil sizes and shapes with ambient light conditions and behavior patterns. *Comp. Biochem. Physiol.* **78A:** 419–426.

CALDWELL, R. L., AND H. DINGLE. 1976. Stomatopods. *Sci. Am.* **234:** 80–89.

DEMOLL, R. 1909. Über die Augen und Augenstielreflexe von *Squilla mantis*. *Zool. Jahrb. Abt. Anat. Ontog.* **27:** 171–212.

HANSTRÖM, B. 1924. Untersuchungen über das Gehirn, insbesondere die Sehganglien der Crustaceen. *Ark. Zool.* **16:** 1–119.

HORRIDGE, G. A. 1978. The separation of visual axes in apposition compound eyes. *Phil. Trans. R. Soc. B* **888:** 1–59.

HORRIDGE, G. A., AND P. DUELLI. 1979. Anatomy of the regional differences in the eye of the mantis *Ciulfina*. *J. Exp. Biol.* **80:** 165–190.

KUNZE, P. 1979. Apposition and superposition eyes. In *Comparative Physiology and Evolution of Vision in Invertebrates, A: Invertebrate Photoreceptors,* H. Autrum, ed. *Handbook of Sensory Physiology* VII/6A: 441–502. Springer-Verlag: Berlin, Heidelberg, New York.

LAND, M. F. 1981a. Optics of the eyes of *Phronima* and other deep-sea amphipods. *J. Comp. Physiol.* **145:** 209–226.

LAND, M. F. 1981b. Optics and vision in invertebrates. In *Comparative Physiology and Evolution of Vision in Invertebrates, B: Invertebrate Visual Centers and Behavior I,* H. Autrum, ed. *Handbook of Sensory Physiology* VII/6B: 471–594. Springer-Verlag: Berlin, Heidelberg, New York.

MANNING, R. B., H. SCHIFF, AND B. C. ABBOTT. 1984. Cornea shape and surface structure in some stomatopod crustacea. *J. Crust. Biol.* **4**(3): 502–513.

MCINTYRE, P., AND A. W. SNYDER. 1978. Light propagation in twisted anisotropic media: application to photoreceptors. *J. Opt. Soc. Am.* **68:** 149–157.

NÄSSEL, D. R. 1975. The organization of the lamina ganglionaris of the prawn, *Pandalus borealis* (Kroyer). *Cell Tissue Res.* **163:** 445–464.

SCHIFF, H. 1963. Dim light vision of *Squilla mantis* L. *Am. J. Physiol.* **205:** 927–940.

SCHIFF, H. 1974. A discussion of light scattering in the *Squilla* rhabdom. *Kybernetics* **14:** 127–134.

SCHIFF, H. 1976. The frequency pattern in the nervous hierarchy of the compound eye of *Squilla mantis* L. (Crustacea, Stomatopoda). *Monit. Zool. Ital.* **10:** 349–379.

SCHIFF, H., B. C. ABBOTT, AND R. B. MANNING. 1985. Possible monocular range-finding mechanisms in stomatopods from different environmental light conditions. *Comp. Biochem. Physiol.* **80**A(3): 271–280.

SCHIFF, H., B. C. ABBOTT, AND R. B. MANNING. 1986a. Optics, range-finding and neuroanatomy in the eye of a mantis shrimp. *Smithsonian Contributions to Marine Sciences.* In press.

SCHIFF, H., AND P. CANDONE. 1986. Superposition and scattering of visual fields in a compound, double eye. II. Stimulation sequences for different distances in a stomatopod from a bright habitat. *Comp. Biochem. Physiol. A.* In press.

SCHIFF, H., F. D'ISEP, AND P. CANDONE. 1986b. Superposition and scattering of visual fields in a compound, double eye. I. Stimulation sequences for different distances in a stomatopod from a dim habitat. *Comp. Biochem. Physiol. A.* In press.

SCHIFF, H., AND A. GERVASIO. 1969. Functional morphology of the *Squilla* retina. *Pubbl. Staz. Zool. Napoli* **37:** 610–629.

SCHIFF, H., AND R. B. MANNING. 1984. Description of a unique crustacean eye. *J. Crust. Biol.* **4**(4): 604–614.

SCHÖNENBERGER, N. 1977. The fine structure of the compound eye of *Squilla mantis* (Crustacea, Stomatopoda). *Cell Tissue Res.* **176:** 205–233.

SHAW, S. R., AND S. STOWE. 1982. Photoreception. In *Neurobiology: Structure and Function,* H. L. Atwood and D. C. Sandeman, eds. *The Biology of Crustacea* **3**: 292–367. Academic Press: New York, London.

SMOLA, U., AND H. WUNDERER. 1981. Fly rhabdomeres twist *in vivo. J. Comp. Physiol.* **142:** 43–49.

SNYDER, A. W. 1979. Physics of vision in compound eyes. In *Comparative Physiology and Evolution of Vision in Invertebrates, A: Invertebrate Photoreceptors,* H. Autrum, ed. *Handbook of Sensory Physiology* VII/**6**A: 225–314. Springer-Verlag: Berlin, Heidelberg, New York.

STRAUSFELD, N. J., AND D. R. NÄSSEL. 1981. Neuroarchitecture of brain regions that subserve the compound eyes of Crustacea and insects. In *Comparative Physiology and Evolution of Vision in Invertebrates, B: Invertebrate Visual Centers and Behavior I,* H. Autrum, ed. *Handbook of Sensory Physiology* VII/**6**B: 1–132. Springer-Verlag: Berlin, Heidelberg, New York.

WEHNER, R. 1981. Spatial vision in arthropods. In *Comparative Physiology and Evolution of Vision in Invertebrates, C: Invertebrate Visual Centers and Behavior II,* H. Autrum, Ed., *Handbook of Sensory Physiology* VII/**6**C: 287–616. Springer-Verlag: Berlin, Heidelberg, New York.